Title Page

Title: RA-Differentiation Enhances Dopaminergic Features, Changes Redox Parameters and Increases Dopamine Transporter Dependency in 6-Hydroxydopamine-Induced-Neurotoxicity in SH-SY5Y cells

Authors: Fernanda M. Lopes[1,2]*, Leonardo L. da Motta[1], Marco A. De Bastiani[1], Bianca Pfaffenseller[1], Bianca W. Aguiar[1], Luiz F. de Souza[3], Geancarlo Zanatta[1], Daiani M. Vargas[1]; Patrícia Schönhofen[1], Giovana F. Londero[1], Liana M. de Medeiros[1], Valder N. Freire[4], Alcir L. Dafre[3], Mauro A. A. Castro[5], Richard B. Parsons[2], Fabio Klamt[1]*.

Filiation: [1]Laboratory of Cellular Biochemistry, Department of Biochemistry, ICBS/UFRGS, 90035-003 Porto Alegre (RS), Brazil; [2]Institute of Pharmaceutical Science, King's College London, 150 Stamford Street, London SE1 9NH, UK; [3]Cellular Defenses Laboratory, Department of Biochemistry, Biological Sciences Centre, Federal University of Santa Catarina (UFSC), 88040-900 Florianopolis (SC), Brazil; [4]Department of Physics at Federal University of Ceará (UFC), 60455-760 Fortaleza (CE), Brazil; [5]Bioinformatics and Systems Biology Laboratory, Federal University of Paraná (UFPR), Polytechnic Center, 81520-260 Curitiba (PR), Brazil.

***Correspondence to:** MSc Fernanda M. Lopes & Prof. Fábio Klamt, PhD Laboratório de Bioquímica Celular (LBC), Departamento de Bioquímica, Instituto de Ciências Básicas da Saúde (ICBS), Universidade Federal do Rio Grande do Sul (UFRGS). 2600 Ramiro Barcelos St., Porto Alegre (RS), Brazil, 90035-003. Phone: +55 51 3308-5556; FAX: +55 51 3308-5535, e-mail: fe.m.lopes@gmail.com / fabio.klamt@ufrgs.br

Abstract

Research on Parkinson's disease (PD) and drug development is hampered by the lack of suitable human *in vitro* models that simply and accurately recreate the disease conditions. To counteract this, many attempts to differentiate cell lines, such as the human SH-SY5Y neuroblastoma, into dopaminergic neurons have been undertaken since they are easier to cultivate when compared to other cellular models. Here we characterized neuronal features discriminating undifferentiated and retinoic acid (RA)-differentiated SH-SYSY cells, and described significant differences between these cell models in 6-hydroxydopamine (6-OHDA) cytotoxicity. In contrast to undifferentiated cells, RA-differentiated SH-SY5Y cells demonstrated low proliferative rate and a pronounced neuronal morphology with high expression of genes related to synapse vesicle cycle, dopamine synthesis/degradation, and of dopamine transporter (DAT). Significant differences between undifferentiated and RA-differentiated SH-SY5Y cells in the overall capacity of antioxidant defenses were found; although RA-differentiated SH-SY5Y cells presented a higher basal antioxidant capacity with high resistance against H_2O_2 insult, they were two-fold more sensitive to 6-OHDA. DAT inhibition by 3α-bis-4-fluorophenyl-methoxytropane and dithiothreitol (a cell-permeable thiol reducing agent) protected RA-differentiated, but not undifferentiated, SH-SY5Y cells from oxidative damage and cell death caused by 6-OHDA. Here we demonstrate that undifferentiated and RA-differentiated SH-SY5Y cells are two unique phenotypes and also have dissimilar mechanisms in 6-OHDA cytotoxicity. Hence, our data support the use of RA-differentiated SH-SY5Y cells as an *in vitro* model of PD. This study may impact our understanding of the pathological

mechanisms of PD and the development of new therapies and drugs for the management of the disease.

Keywords SH-SY5Y cells; retinoic acid; Parkinson's disease; experimental model; 6-hydroxydopamine; dopamine transporter.

Acknowledgements

Brazilian funds CNPq/MS/SCTIE/DECIT - Pesquisas Sobre Doenças Neurodegenerativas (#466989/2014-8), MCT/CNPq INCT-TM (#573671/2008-7), and Rapid Response Innovation Award/MJFF (#1326-2014) provided the financial support without interference in the ongoing work. FK received a fellowship from MCT/CNPq (#306439/2014-0). FML received a fellowship from Programa de Doutorado Sanduíche no Exterior - PDSE/CAPES (#14581/2013-2). We thank Dr. Florencia M. Barbé-Tuana for technical assistance with flow cytometry, and Dr. Tadeu Mello e Souza for kindly providing DATi.

Introduction

Dopaminergic degeneration found in Parkinson's disease (PD) (Gibb 1991) is mainly associated with oxidative stress (Fariello 1988) and mitochondrial dysfunction (Schapira et al. 1990). However, the functional changes operating during the initial stage of PD remain unknown (Mullin and Schapira 2015). The lack of understanding the molecular mechanisms of PD has many causes (Olanow et al. 2008; Olanow 2009), which one of them is attributed to the difficulty to reproduce the complex physiological features of a human dopaminergic neuron *in vitro* (Schüle et al. 2009; Bal-Price et al. 2010). Hence, there are limited reliable neuronal *in vitro* cell models to study PD pathophysiological mechanisms (Radio and Mundy 2008; Haggarty and Perlis 2014).

In this context, the human neuroblastoma cell line SH-SY5Y is the most used *in vitro* model of dopaminergic neurons (Xie et al. 2010) because not only it expresses the catecholamine synthesis machinery, but also it is easy to cultivate when compared with another *in vitro* models (*e.g.* primary culture and inducible pluripotent stem cells –iPS) (Biedler et al. 1978; Kovalevich and Langford 2013). Even though these cells are widely used in PD research, they are epithelial cells and do not present neuronal properties such as a terminal post-mitotic state and the expression of synaptic proteins (Radio and Mundy 2008). Interestingly, the *in vitro* differentiation induced by retinoic acid (RA) of this cell line into a neuron-like phenotype was established more than 30 years ago (Påhlman et al. 1984).

However, there is no consensus which differentiation protocol is more suitable for this cells line. The scientific literature shows a divergence not only in

serum concentration (1-10% FBS), which neurotrophin to be used (*e.g.* RA, BDNF, TPA), but also in differentiation length (4-12 days). Hence, depending on the protocol used, there are several discrepancy among findings regarding neuronal and dopaminergic markers (*e.g*. tyrosine hydroxylase –TH and dopamine transporter –DAT) (Presgraves et al. 2004; Cheung et al. 2009; Agholme et al. 2010; Lopes et al. 2010; Korecka et al. 2013). This brings discussion whether SH-SY5Y cells must be differentiated (Luchtman and Song 2010; Xie et al. 2010).

Furthermore, different protocols also may cause changings in cell susceptibility to neurotoxins, such as 6-hydroxydopamine (6-OHDA) (Cheung et al. 2009; Lopes et al. 2010; Forster et al. 2016). *In vivo*, it is widely accepted that this toxin enters into the dopaminergic neuron *via* DAT and causes a massive oxidative stress (Ljungdahl et al. 1971). However, 6-OHDA mechanism of action is still controversial for *in vitro* studies. Although DAT inhibitors provide a partial protection against 6-OHDA toxicity towards primary dopaminergic neurons (Cerruti et al. 1993; Abad et al. 1995), many lines of evidence showed no protection in undifferentiated SH-SY5Y cells from cell death induced by this toxin (Storch et al. 2000; Izumi et al. 2005; Hanrott et al. 2006). Regarding RA-differentiated SH-SY5Y cells, no study showed the effect of DAT inhibition in 6-OHDA-induced cell death.

Even though with the emergence of new, more physiologically relevant models such as iPS as *in vitro* models for PD (Hartfield et al. 2014), it is clear that the majority of studies have been undertaken using cell lines such as SH-SY5Y due to considerations such as availability of iPS and the necessary expertise in their differentiation into dopaminergic neurons (Filograna et al.

2015; Forster et al. 2016; Lin and Tsai 2016). Hence, an understanding of the potential differences in SH-SY5Y cell line RA-differentiated and undifferentiated states and their response to 6-OHDA are imperative as this remains the most commonly-used *in vitro* model (Kovalevich and Langford 2013).

In the present work, we aimed to validate a differentiation protocol previously described by our research group (Lopes et al. 2010) comparing undifferentiated and RA-differentiated SH-SY5Y cells regarding gene expression of important cellular networks related to dopaminergic neuronal machinery, morphology, redox metabolism and 6-OHDA cytotoxicity. To further investigate 6-OHDA operating mechanisms in both models, DAT inhibition and pre-treatment with thiol reducing agents were performed. Here we demonstrate critical differences between models, such as DAT dependency of 6-OHDA-induced cell death in RA-differentiated SH-SY5Y cells.

Materials and Methods

Cell Culture

Human neuroblastoma cell line SH-SY5Y (ATCC, Manassas, VA, USA) was maintained in a 1:1 mixture of Ham's F12 and Dulbeco Modified Eagle Medium (DMEM) supplemented with 10% heat-inactivated fetal bovine serum (FBS) (Cripion®, São Paulo, SP, Brazil), 2 mM of glutamine, 100 U/mL of penicillin/streptomycin and antimycotic (Thermo Fisher Scientific®, cat. #10378016, Waltham, MA, USA) in a humidified atmosphere of 5% of CO_2 at 37ºC.

In our cellular differentiation protocol (as described in Fig.1) only attached cells were maintained and floating cells were discarded. 3 $X10^4$ cells/cm^2 were seed in 10% FBS medium. After 24 hours (day 1), medium was

replaced with medium in which the FBS concentration was reduced to 1% and supplemented with 10 µM of RA (all-trans-retinoic-acid, Enzo® - East Farmingdale, NY, USA), and incubated for 7 days. At the day 4, the medium was replaced, and at the day 7, cells were harvested and used for experiments.

It is important to note that successful differentiation depends upon (at least) 3 factors: (*i*) the confluence of the cells in day 1 must be around 75% (higher confluence inhibits neurite outgrowth, and lower confluence leads SH-SY5Y cells to detach); (*ii*) the cell medium should only be used for a maximum of 2 weeks to avoid glutamine decomposition; and (*iii*) RA powder is diluted in absolute ethanol to prepare the stock solution. The concentration of this solution was determined using E^M (351 nm) = 45000 at the day of the medium replacement (*i.e.* days 1 and 4) to control any changes in the concentration that may occur during storage (Lopes et al. 2010; Sharow et al. 2012).

RNA isolation and microarray assay

Cells were harvested and the RNA was isolated using TRIzol Reagent (Thermo Fisher Scientific®, Waltham, MA, USA) following by purification (Qiagen RNeasy Mini Kit #74 104 and #79 254 - Free RNase DNase Set Qiagen,Hilden, Germany). Microarray analysis was performed using the chip GeneChip® PrimeView™ Human Gene Expression Array (Affymetrix™). The samples were collected at the day 0 (undifferentiated cells) and day 7 (RA-differentiated cells) (Fig. 1) and raw data was deposited on GEO repository (GEOID: GSE71817).

Gene Set Enrichment Analysis (GSEA) and expression values

Four genes networks were analyzed in both undifferentiated and RA-differentiated SH-SY5Y cells: cell cycle, synapse vesicle cycle, dopaminergic synapse and antioxidant (extracted from KEGG platform)

(Http://www.genome.jp/kegg/pathway.html 2016). Gene set enrichment analysis was used to identify genes that contribute to global changes in expression levels in a given microarray dataset comparison. GSEA considers experiments with genome-wide expression profiles from two classes of samples (*e.g.* RA-differentiated cells *vs.* undifferentiated). Genes were ranked based on the correlation between their expression and the class distinction. Given *a prior* defined network (*e.g.* synaptic vesicle cycle), the GSEA determines if the members of these sets of genes are randomly distributed or primarily found at the top or bottom of the ranking (Subramanian et al. 2005).

To access the logarithm of gene expression, raw CEL files were analyzed using the R/Bioconductor pipeline. The data was normalized by Robust Multi-array Average (RMA) using the AFFY package, log (base 2) transformed, and batch-corrected with ComBat using the SVA package.

Cell cycle and cellular growth

DNA composition was measured using propidium iodide (PI) (Thermo Fisher Scientific®, cat. # P3566, Waltham, MA, USA), flow cytometry (BD Accuri™ C6 Flow Cytometer, USA). The results were express as percentage of cells in each cell cycle phase (G0/G1, S, G2/M). Cellular proliferation was measured by cell counting using a Neubauer Chamber. Undifferentiated cells reach the confluency at the day 4, forming a monolayer. After this, cells continued to proliferate, as shown in Fig. 2a, but as floating cells.

Neurite Density

Neurite density was evaluated by immunofluorescence. Cells were washed with PBS, fixed with methanol/acetone solution (1:1) for 20 minutes in room temperature and permeabilized with PBS/Tween 0,2%. The blocking was performed with 1% BSA solution for 1 h in room temperature. Then, cells were

incubated with anti-βIII tubulin antibody (Alexa 488-conjugated – Abcam®, cat. # ab204605, Cambridge, UK, - dilution: 1:250) for 2 hours in room temperature and with Nuclear dye DAPI (Thermo Fisher Scientific®, cat. # D1306, Waltham, Massachussets, USA- dilution: 0.25 µg/µL) for 5 min. Randomly selected Images were captured using an Olympus IX70 inverted microscope and analyzed with NIS-elements software. Neurite density was assessed using the AutoQuant Neurite software (implemented in *R*), and expressed as arbitrary units (A.U.) (Schönhofen et al. 2015).

Dopamine immunoreactivity

Dopamine reactivity was evaluated using an anti-dopamine antibody (Abcam®, cat. # ab6427, Cambridge, UK dilution: 1:250) followed by incubation with Alexa 488-conjugated-antibody (Thermo Fisher Scientific®, cat. #A11008, Waltham, MA, USA- A11008 - dilution: 1:500). Randomly selected images were captured using an EVOS® FLoid® Cell Imaging (Korecka et al. 2013).

Cytotoxicity parameters

Undifferentiated and RA-differentiated SH-SY5Y cells were treated for 24 hours with 6-OHDA and H_2O_2. Cell viability were analyzed using 3-(4,5-dimethylthiazol-2-yl)-2,5-diphenyltetrazolium bromide (MTT- Sigma®, cat. # M5655) reduction assay as previously described (Lopes et al. 2010).

Oxidative stress parameters

We evaluated the redox status in both undifferentiated and RA-differentiated SH-SY5Y cells by measuring: reduced thiol and reduced glutathione (GSH) levels as well as the following antioxidant enzymes activities: Glutathione Peroxidase (GPx), Catalase (CAT), Superoxide Dismutase (SOD), Thioredoxin Reductase (TrxR), Glutathione Reductase (GR), Glutathione-S-transferase (GST) as described previously (Lopes et al. 2012). H_2O_2 generation

was measured using AmplexRed® (Thermo Fisher Scientific®, cat. # a12222, Waltham, MA, USA).

Reducing thiol agents treatment

The role of reducing agents in 6-OHDA-cytotoxicity was assessed *via* pre-treatment with Dithiothreitol (DTT)(Sigma®, cat. # D0632) or *tris*(2-carboxyethyl)phosphine (TCEP) (Sigma®, cat. # C4706) in both cell models for 1 hour in 37ºC. Cells were then incubated with the median toxic dose (TD_{50}) dose of 6-OHDA. The cytotoxicity was analyzed using MTT reduction.

DAT immunocontent

To evaluate changes in DAT immunocontent during the RA-differentiation process, western blot analysis was performed using anti-DAT antibody (Santa Cruz® Biotechnology, cat. # 9299, Dallas, TX, USA - dilution: 1:1000) and rabbit anti-glyceraldehyde-3-phosphate dehydrogenase (GAPDH) antibody (Abcam®, cat. # ab9485, Cambridge, UK - dilution 1:5000) as loading control.

Molecular Docking

The calculations performed in this study have taken full advantage of the X-ray crystal structure of the *Drosophila melanogaster* DAT (PDB ID 4M48) at 3.0 Å of resolution (Penmatsa et al. 2013).

Molecular docking was performed using Autodock4 and the protocol adopted validated through the redocking of nortriptyline in the DAT binding site, as describe elsewhere (Halperin et al. 2002; Mohammad et al. 2008), which was employed to obtain the molecular structures of dopamine, 6-OHDA, *p*-quinone and DATi (DATi = 3α-bis-4-fluorophenyl-methoxytropane) (Tocris®, cat. #0918, Avonmonth, Bristol, UK) for docking input. Upon completion, a thousand poses were obtained (50 poses per output) and clustered within a RMSD tolerance of 1.0 Å using Autodock Tools The best results obtained were based

upon visual inspection and the calculated binding energy. Binding energy (E_{OPT}) was recalculated, using Forcite code, through the equation "E_{OPT} = EDAT + L - (EDAT + EL)" where EDAT + L is the total energy of the system formed by ligand bond in DAT; EDAT is the total energy of the DAT alone, while EL is the total energy of the ligand molecule alone.

DAT pharmacological inhibition

To investigate the DAT dependency of 6-OHDA-induced cell death in both models, cells were pre-incubated for 30 minutes with 20 µM of DATi (Tocris®, cat. #0918, Avonmonth, Bristol, UK). Following this, cells were exposure to TD_{50} 6-OHDA for 24 hours (Lopes et al. 2010). Cell viability was assessed using MTT assay. H_2O_2 generation was measured using AmplexRed®.

Statistical Analysis

Data were expressed as means ± S.D of at least 3 independent experiments carried out in triplicate, and P-values were considered significant for $p < 0.05$. Differences within the experimental groups were determined by Student's *t*-test or one-way analysis of variance (ANOVA). Comparison among means was carried out using Newman-Keuls multiple comparisons test as *post hoc* (GraphPad® Software 5.0).

Results

RA-differentiation protocol induces neuronal features in SH-SY5Y cells

PD-target cells are neurons derived from *substantia nigra pars compacta*, which are specialized cells that process and transmit information through electrical and chemical synapses, with stellate morphology and do not undergo to cell divisions (Kandel 2013). To evaluate these relevant features to mimic more accurately the neuronal cell physiology, we explored the effect of RA-

differentiation protocol on cell growth, morphology and the expression of gene sets associated with cell cycle and synapse vesicle cycle (protocol description in Fig. 1).

Here we showed a significant decrease in the proliferation rates of RA-differentiated SH-SY5Y cells (Fig. 2a) ($n = 3$; $p < 0.001$) mainly associated with a decrease in S phase in combination with an arrest in G2-M (Fig. 2b) ($n = 3$; $p < 0.001$). Further, we investigated gene expression of the cell cycle network (KEGG pathways entry #hsa04110) using microarray analysis in undifferentiated and RA-differentiated cells. Although no statically significant differences were observed between the two phenotypes, there are genes associated with G2-M arrest, such as *GDD45G* and *SMAD3* (Herrup and Yang 2007), upregulated in RA-differentiated SH-SY5Y cells as shown in Supplementary Fig. 1 (Electronic Supplementary Material).

Upon the decrease in proliferation rate and cell cycle arrest, a significant change in morphology with increased neurite density was verified in RA-differentiated cells (Fig. 2c,d) ($n = 3$; $p < 0.0001$), suggesting a change from epithelial (as defined by ATCC for SH-SY5Y cells) (www.atcc.org/Products/All/CRL-2266.aspx) to a stellate neuronal morphology. After morphological characterization, we analyzed which cellular model possessed the appropriate molecular machinery to support the synaptic transmission, using the synaptic vesicle cycle gene list (extracted from KEGG pathways entry #hsa04728). We found a significant enrichment of this gene set in RA-differentiated, compared to undifferentiated, SH-SY5Y cells (Fig. 2e,f) ($n = 4$; $p < 0.05$). Enriched genes are listed in Table 1.

RA differentiation potentiates dopaminergic features in SH-SY5Y cells

After studying the differences in general neuronal properties obtained with from RA-differentiation protocol, we investigated dopaminergic features of both phenotypes of SH-SY5Y cells. At first, we evaluated global differences in gene expression of the dopaminergic synapse network, where we found no significant differences between the two models (Fig. 3a). However, there are genes upregulated in RA-differentiated cells listed in Supplementary Table 1, (Electronic Supplementary Material).

Using differential gene expression analysis, we verified the expression levels of the most common dopaminergic markers (Korecka et al. 2013), associated with catecholamine synthesis (Dopa decarboxylase- *DDC*, GTP cyclohydrolase- *GCH1* and *TH*), degradation (monoamine oxidase A and B - *MAOA, MAOB-,* Catechol-O-methyltransferase-*COMT*), and synaptic function (Vesicular monoamine transporter 1 and 2- *SLC18A1*, *SLC18A2*, dopamine transporter- *SLC6A3*, dopamine receptor D2- *DRD2*). Both models present the same level of expression in all genes studied except for *DR2*, *GHC* and *SLC18A1,* which have higher expression in the RA-differentiated cells (Fig. 3b).

Lastly, dopamine immunocontent was investigated using an immunocytochemical approach in both SH-SY5Y phenotypes. In Figure 3c, we confirmed that both models have immunochemical detection of this neurotransmitter. Hence, in spite of both models of SH-SY5Y cells present dopamine content, neuronal dopaminergic features are potentiated after RA-differentiation (*e.g DRD2* and *SLC18A1*).

RA-differentiation induces changes in oxidative status and 6-OHDA-mediated neurotoxicity in SH-SY5Y cells

Due to the pivotal role played by reactive species in PD (Fariello 1988), the endogenous machinery responsible for the basal redox status should be

characterized when establishing any relevant *in vitro* cell model of PD. To do so, we firstly evaluated the gene expression levels of the human antioxidant network (according to KEGG pathways). There were no differences in gene expression in antioxidant network. However, some antioxidant genes were upregulated in RA-differentiated cells (*e.g. GPX3, TMX4 and GRLX*) (Fig. 4a).

To better characterize these redox differences, we evaluated the activity of several enzymes involved in first line antioxidant defenses and the level of non-enzymatic antioxidant defenses in both SH-SY5Y phenotypes. Our *in vitro* validation revealed that RA-differentiated cells have higher antioxidant enzymes activities and lower levels of H_2O_2 production (Table 2).

After investigate the basal redox metabolism in undifferentiated and RA-differentiated SH-SY5Y cells, we aimed to examine their susceptibility to oxidative stress induced by H_2O_2 and 6-OHDA. RA-differentiated SH-SY5Y cells were more resistant to H_2O_2, yet they were two-fold more susceptible to 6-OHDA cytotoxicity (Table 2). It is well known that 6-OHDA toxicity acts *via* the induction of oxidative stress, however the higher endogenous antioxidant capacity observed was not able to protect RA-differentiated cells from the cell death, suggesting a dissimilar mechanism of 6-OHDA detoxification in this cellular model.

The role of thiols in 6-OHDA-induced cell death in undifferentiated and RA-differentiated SH-SY5Y cells

Previous data have shown that 6-OHDA uptake is not an essential process and the auto-oxidation occurs extracellularly in undifferentiated SH-SY5Y cells (Storch et al. 2000; Hanrott et al. 2006; Iglesias-González et al. 2012), suggesting that this toxin has different mechanisms from animal and

primary culture models. Hence, in order to understand our previous results regarding the susceptibility of 6-OHDA in RA-differentiated cells, we evaluate the role of cell-permeable and cell-impermeable reducing agents in 6-OHDA-induced-cell-death.

We first pre-incubated undifferentiated and RA-differentiated cells with two thiol reducing agents TCEP (a cell-impermeable compound) and DTT (a cell-permeable molecule), before challenging cells with 6-OHDA (Fig. 4b,d) (Hsu et al. 2005). Interestingly, no differences were found between both cellular models when TCEP were used to protect cells against 6-OHDA-oxidant insult (Fig. 4c). On the other hand, DTT was able to prevent 60% of 6-OHDA-dependent cytotoxicity in RA-differentiated cells (Fig. 4e) ($n = 3$; $p < 0.0005$), in contrast to only 24% in undifferentiated cells, indicating that, in RA-differentiated cells, an intracellular oxidation step of the neurotoxin is associated with the cell death caused by 6-OHDA (Fig 4b, $F(3,8) = 126.5$, n = 3; $p < 0.0001$).

The role of DAT in 6-OHDA-induced-cell death in undifferentiated and RA-differentiated SH-SY5Y cells

To investigate more accurately the role of intracellular auto-oxidation, we evaluated the role of DAT in the toxicity induced by 6-OHDA in both cellular models because the activity of this transporter is fundamental for toxin uptake. In Figure 5a shows an increase in DAT immunocontent in RA-differentiated cells ($n = 3$; $p < 0.01$).

We then verified whether the inhibition of this transporter interfered in the cell death caused by 6-OHDA. First, we examined how DATi and 6-OHDA interacts with DAT by using molecular docking followed by classical refinement of geometries (Fig. 5b), and compared the binding energy (E_{OPT}) of those

compounds with the corresponding values obtained for dopamine and *p*-quinone (Supplementary Fig. 2 and Supplementary Table 2 for the raw docking data in Electronic Supplementary Material). Our data suggests that DATi inhibits DAT by preventing substrate binding and stabilizing the outward-open conformation. Furthermore, we found that dopamine, DATi, *p*-quinone and 6-OHDA, all compete sterically for the same binding site *via* the spatial blockage of Asp46 residue (Asp79 in DAT from *Homo sapiens*). This steric blockage of the same binding site demonstrates a competitive inhibition mechanism of action for DATi (Fig. 5b). Due to the lower ligation energy of DATi for DAT in comparison to *p*-quinone and 6-OHDA, but higher for dopamine, our docking data showed that DATi blocks completely the interaction of dopamine with DAT, but only partially *p*-quinone and 6-OHDA (Supplementary Table 2 in Electronic Supplementary Material). Thus, it suggests that DATi inhibits DAT by preventing substrate binding and stabilizing the outward-open conformation.

Based on these findings, we pharmacologically inhibited DAT in both cellular models *via* incubation with DATi prior to challenging cells with 6-OHDA. Our data showed that DAT inhibition resulted in a significant decrease in cell death (41%) (Fig. 5f) and H_2O_2 production (48%) (Fig. 5d) by 6-OHDA treatment only in RA-differentiated cells with no effect observed in undifferentiated cells, suggesting a specific role played by DAT in the cell death caused by this neurotoxin in the neuronal phenotype (Fig. 5c, $F(3,12) = 9.571$, n =3; $p < 0.01$) (Fig. 5e, $F(3,8) = 201.4$, n = 3; $p < 0.0001$).

Discussion

The difficulty in mimicking neuronal features *in vitro* has always been an issue in neurosciences studies, thus the development of more suitable models

is necessary since they are fundamental to study molecular mechanism of neurodegenerative disease, such as PD. In this regard, the most *in vitro* experimental model used for PD is the human neuroblastoma SH-SY5Y cell because they express dopaminergic markers and are easy to cultivate when compared to other models (Xie et al. 2010; Kovalevich and Langford 2013). We previously established a catecholaminergic differentiation protocol for this cell line (Lopes et al. 2010). Here we focused in explore neuronal features in both cellular models.

There are many lines of evidence showing the effect of RA-differentiation in SH-SY5Y regarding the evaluation of proliferation rates (Ross 1996; Pezzini et al. 2016; Kunzler et al. 2016). Previous studies have demonstrated that RA-induced differentiation can cause cell cycle arrest either in G1/G0 phase or in G2/M phase and a decrease in proliferation rates, which leads to terminal differentiation of neuroblastoma cells (Qiao et al. 2012; Hämmerle et al. 2013).

We verified decreased cellular growth in RA-differentiated cells was associated with a decrease in S phase in combination with G2-M arrest (Fig. 2b). This data corroborates with our findings regarding gene expression of the cell cycle network. Genes upregulated in RA-differentiated cells are associated with cell cycle arrest, for instance, cyclin-dependent protein kinases (CDK) inhibitors (*e.g.* p18, p19, p21 and p27) and to G2-M arrest, such as *GDD45G* and *SMAD3* (Herrup and Yang 2007) (Summarized in Supplementary Fig. 1 in Electronic supplementary material). Moreover, the cell cycle arrest in G2-M is commonly found in neurodegenerative diseases such and PD, where some populations of neurons complete DNA synthesis and are able to pass through the S phase, but are arrested at the G2/M (Frade and Ovejero-Benito 2015).

Another important neuronal parameter is cellular morphology. Neurons present neurites, which refers to axons and dendrites extended by neuronal cell lines, thus their quantification is an important morphological parameter of neuronal differentiation (Radio and Mundy 2008; Bal-Price et al. 2010). Here, we showed an increase in neurite density in RA-differentiated cells, representing a significant advantage of this cellular model, since these structures form synapses and can be used as an endpoint in neurotoxicological evaluations (Lopes et al. 2012).

Besides low proliferation rates and stellate morphology, dopaminergic neuronal cells process their information through chemical synapses. The biological event related to neurotransmitter release is the synaptic vesicle cycle (Kandel 2013). This pathway consists of exocytosis followed by endocytosis and recycle (Rizo and Xu 2015). At first, vesicles are loaded with neurotransmitters, which require the presence of an active transporter along with a proton pump to provides the required pH and electrochemical gradients. Fundamental to this is the role of H^+-ATPase transporters and solute carriers such as *SLC18A1*, *SLC18A3* and *SLC17A8* (Beyenbach and Wieczorek 2006). Once the vesicles are loaded, they are tethered near to the release sites, after which vesicles are primed before being ready to undergo fusion. Genes involved in this process include *UNC13*, *RIMS1* and syntaxin (Madison et al. 2005). The primed vesicles subsequently undergo fusion processes that are regulated by SNARE proteins, such as SNAP-25, NSF and complexins (Hu et al. 2002). Finally, the synaptic vesicles incorporated to the plasma membrane are retrieved by endocytosis, a process which involves many proteins, *e.g.* dynamins and clathrins (Takei et al. 1996). Our results demonstrated that all of

these genes were up-regulated in RA-differentiated cells (Fig. 2e,f; Table 1), suggesting that this model has appropriate machinery to support synapses.

Our data point to highly diverse phenotypes presented by both cellular models. Undifferentiated cells exhibited characteristics typical of a tumoral phenotype, namely epithelial morphology and high proliferation rates. In contrast, RA-differentiated SH-SY5Y cells were characteristic of a neuronal phenotype, presenting low proliferation rates, a pronounced neuronal morphology and an enrichment of the molecular machinery responsible for synaptic function.

After neuronal characterization, we aimed to verify if both cellular models have dopaminergic phenotype, since these cells are the most affected neurons in PD. Here, we demonstrated that both phenotypes of SH-SY5Y cells expressed the dopaminergic machinery. This was expected since it is well known that neuroblastoma cancers (as the primary tumor that SH-SY5Y cells were isolated from) produce catecholamines, mainly because they have low levels of dopaminergic markers (Howman-Giles et al. 2007). As such, undifferentiated cells are commonly used as PD model (Xie et al. 2010).

Previous data showed that the differentiation process does not lead to increase of dopaminergic markers in SH-SY5Y cells, which it brings the discussion whether they need to be differentiated (Luchtman and Song 2010). On the other hand, many lines of evidence showed that RA-differentiated cells increase their expression of these dopaminergic markers, such as TH and DAT (Påhlman et al. 1984; Lopes et al. 2010; Filograna et al. 2015). These discrepancies in the literature might be attributable to the varying differentiation protocols used, since there are differences between them, such as duration, cell

densities, serum concentration and differentiation agent (*e.g.* RA, staurosporine, BDNF) (Cheung et al. 2009; Agholme et al. 2010; Lopes et al. 2010; Filograna et al. 2015).

Hence, our results show that both models have the machinery necessary to synthetize and release dopamine. Although no global statistically significant differences were observed between the two phenotypes, there are genes associated with dopamine synthesis regulation (*PKA*, *MAPK*, *CAMKII* and *PP2A*) significantly upregulated in RA-differentiated SH-SY5Y cells (Fig. 3a; Supplementary Table 1) (Dunkley et al. 2004; Daubner et al. 2011). Moreover, differential expression showed significant increase in GHC1, *DRD2* and *SLC18*, three important catecholaminergic markers. These findings demonstrated that RA –differentiation potentiates the dopaminergic phenotype, which validates our protocol and its potential use as PD *in vitro* model.

Since dopaminergic neurons are exposed to a chronic oxidative damage, mostly attributed to the high levels of iron present in SNpc, the hydroxyl radical ($HO^{\bullet}$) produced by dopamine metabolism (Zhou et al. 2010), oxidative stress is thought to causally contribute to the pathogenesis of progressive neurodegeneration observed in PD (Fariello 1988). Hence, oxidative stress parameters should be investigate when establishing *in vitro* cell model of PD. Our *in vitro* validation revealed that both models have thioredoxin and glutathione antioxidant systems as the main antioxidant defense. The H_2O_2 detoxification in neuronal cells is catalyzed primarily by thioredoxin and glutathione systems, which are the most important antioxidants in the brain (Lopert et al. 2012; Garcia-Garcia et al. 2012), hence we found that both models mimic the oxidative neuronal profile.

Moreover, we showed that RA-differentiated cells presented a higher basal antioxidant capacity and decrease of H_2O_2 production. At first, these data seem controversial because neuronal cells presents low antioxidant levels (Halliwell 2006; Dexter and Jenner 2013), hence the differentiated cells do not represent accurately the physiology of dopaminergic neurons. However, here we are comparing the neuronal and tumoral phenotypes. The oxidative environment of the undifferentiated cells could be explained by its proliferative profile since H_2O_2 is fundamental for cellular growth (Policastro et al. 2004; Sies 2014).

Here the most intriguing observation was that RA-differentiated SH-SY5Y cells were more resistant to H_2O_2, yet were more susceptible to 6-OHDA cytotoxicity (Table 2). Cellular resistance to H_2O_2 in the neuronal phenotype can be explained by the elevated basal antioxidant capacity. Since the RA-induced differentiation decreases levels of TrxR and GSH, this may suggests a role of these antioxidants in 6-OHDA detoxification, as previously described (Soto-Otero et al. 2000; Lopert et al. 2012). Hence, the resistance to 6-OHDA found in undifferentiated cells can be explained, at least in part, by the high GSH levels presented in the tumoral phenotype.

It is widely elucidate that 6-OHDA is taken up by dopaminergic neurons *via* DAT (Tranzer and Thoenen 1973) and auto-oxidation process occurs intracellularly (Glinka et al. 1997) manly because the toxicity can be blocked by DAT inhibition (González-Hernández et al. 2004). On the other hand, previous data have shown that 6-OHDA uptake is not an essential process and the auto-oxidation occurs extracellularly in undifferentiated cells (Izumi et al. 2005). Here we found that part of the oxidative dysfunction caused by 6-OHDA involves the

uptake of the neurotoxin (or some metabolite, such as *p*-quinones) presumably followed by intracellular auto-oxidation in RA-differentiated cells.

Further investigation about intracellular oxidation demonstrated that pharmacological DAT inhibition decreases H_2O_2 production and cellular death caused by 6-OHDA only in RA-differentiated SH-SY5Y cells. Regarding undifferentiated SH-SY5YS cells, DAT inhibition did not protect the cells, possibly because these cells have low levels of DAT (Presgraves et al. 2004), which corroborates with previous results (Storch et al. 2000; Izumi et al. 2005).

These results may impact the development of new therapies and drugs for the management of the disease. To date, PD is still an incurable disease and we have failed to find neuroprotective compounds (Olanow et al. 2008). The main reason to this issue is the lack of understanding of the initial steps underlying dopaminergic degeneration (Obeso et al. 2010). Although PD is considered a complex disorder where many mechanisms are involved (*e.g.* protein aggregation, mitochondria dysfunction and oxidative stress), the common pathology found in all PD cases is the dopaminergic degeneration (Gibb 1991). Hence, the development of better dopaminergic cell models and the understanding of dopaminergic cell physiology are essential for PD research. In spite of many lines of evidence have shown that undifferentiated SH-SY5Y cells are dopaminergic-producing cells and easy to cultivate (Presgraves et al. 2004; Cheung et al. 2009; Agholme et al. 2010; Lopes et al. 2010), they do not reproduce both dopaminergic physiology and 6-OHDA-induced-cell death mechanisms of *in vivo* or primary cell culture studies. Thus, SH-SY5Y cells are the target of many discussions whether it should be used in PD research. Our data suggests, for the first time, the role of toxin uptake by

DAT in RA-differentiated cells, showing that an easy cellular model can mimic, at least part, 6-OHDA-induced cell death *in vivo*.

Conclusions

Undifferentiated and RA-differentiated SH-SY5Y cells are two unique phenotypes which can be distinguished by differences found in cells morphology, cell growth, neuronal and dopaminergic marker expression and redox metabolism. These features may contribute towards two different mechanisms of action for 6-OHDA-cytotoxicty observed in both models. In the neuronal phenotype, we demonstrated DAT dependency in 6-OHDA-induced cell death, which is likely related to their dopaminergic phenotype. Many previous studies have used undifferentiated cells as a PD model to study molecular mechanisms, to test potential drugs for the treatment of this disease and also to evaluate 6-OHDA's mechanisms of action and cellular targets. However, our data demonstrate that undifferentiated cells does not possess neuronal properties, which can create significant bias in such studies, and may have contributed, at least in part, to the limitations in our understanding of PD pathophysiology and, consequently, the lack of potential drugs to treat the disease. Hence, our data support the use of RA-differentiated cells as an *in vitro* model of PD.

Conflict of interests

The authors declare that they have no competing interests.

Author Contributions Statement

F.M.L., L.L.M, L.F.S, D.M.V, P.S., G.F.L. and L.M performed experiments. B.P. and B.W.A performed the RNA extraction for the microarray analysis, G.Z. and V.N.F. performed the molecular docking. F.M.L, L.L.M,

M.A.D.B, M.A.A.C., R.B.P., A.L.D. and F.K. analyzed and interpreted the data.

F.M.L, and F.K. conceived and designed the experiments. F.M.L and F.K. wrote the manuscript.

References

Abad F, Maroto R, López MG, et al (1995) Pharmacological protection against the cytotoxicity induced by 6-hydroxydopamine and H2O2 in chromaffin cells. Eur J Pharmacol 293:55–64.

Agholme L, Lindström T, Kågedal K, et al (2010) An in vitro model for neuroscience: differentiation of SH-SY5Y cells into cells with morphological and biochemical characteristics of mature neurons. J Alzheimers Dis 20:1069–82. doi: 10.3233/JAD-2010-091363

Bal-Price AK, Hogberg HT, Buzanska L, Coecke S (2010) Relevance of in vitro neurotoxicity testing for regulatory requirements: challenges to be considered. Neurotoxicol Teratol 32:36–41. doi: 10.1016/j.ntt.2008.12.003

Beyenbach KW, Wieczorek H (2006) The V-type H+ ATPase: molecular structure and function, physiological roles and regulation. J Exp Biol 209:577–89. doi: 10.1242/jeb.02014

Biedler JL, Roffler-Tarlov S, Schachner M, Freedman LS (1978) Multiple neurotransmitter synthesis by human neuroblastoma cell lines and clones. Cancer Res 38:3751–7.

Cerruti C, Walther DM, Kuhar MJ, Uhl GR (1993) Dopamine transporter mRNA expression is intense in rat midbrain neurons and modest outside midbrain. Brain Res Mol Brain Res 18:181–6.

Cheung Y-T, Lau WK-W, Yu M-S, et al (2009) Effects of all-trans-retinoic acid on human SH-SY5Y neuroblastoma as in vitro model in neurotoxicity research. Neurotoxicology 30:127–35. doi: 10.1016/j.neuro.2008.11.001

Daubner SC, Le T, Wang S (2011) Tyrosine hydroxylase and regulation of dopamine synthesis. Arch Biochem Biophys 508:1–12. doi: 10.1016/j.abb.2010.12.017

Dexter DT, Jenner P (2013) Parkinson disease: from pathology to molecular disease mechanisms. Free Radic Biol Med 62:132–44. doi: 10.1016/j.freeradbiomed.2013.01.018

Dunkley PR, Bobrovskaya L, Graham ME, et al (2004) Tyrosine hydroxylase phosphorylation: regulation and consequences. J Neurochem 91:1025–43. doi: 10.1111/j.1471-4159.2004.02797.x

Fariello RG (1988) Experimental support for the implication of oxidative stress in the genesis of parkinsonian syndromes. Funct Neurol 3:407–12.

Filograna R, Civiero L, Ferrari V, et al (2015) Analysis of the Catecholaminergic Phenotype in Human SH-SY5Y and BE(2)-M17 Neuroblastoma Cell Lines upon Differentiation. PLoS One 10:e0136769. doi: 10.1371/journal.pone.0136769

Forster JI, Köglsberger S, Trefois C, et al (2016) Characterization of Differentiated SH-SY5Y as Neuronal Screening Model Reveals Increased Oxidative Vulnerability. J Biomol Screen. doi: 10.1177/1087057115625190

Frade JM, Ovejero-Benito MC (2015) Neuronal cell cycle: the neuron itself and its circumstances. Cell Cycle 14:712–20. doi: 10.1080/15384101.2015.1004937

Garcia-Garcia A, Zavala-Flores L, Rodriguez-Rocha H, Franco R (2012) Thiol-redox signaling, dopaminergic cell death, and Parkinson's disease. Antioxid Redox Signal 17:1764–84. doi: 10.1089/ars.2011.4501

Gibb WR (1991) Neuropathology of the substantia nigra. Eur Neurol 31 Suppl 1:48–59.

Glinka Y, Gassen M, Youdim MB (1997) Mechanism of 6-hydroxydopamine neurotoxicity. J Neural Transm Suppl 50:55–66.

González-Hernández T, Barroso-Chinea P, De La Cruz Muros I, et al (2004) Expression of dopamine and vesicular monoamine transporters and differential vulnerability of mesostriatal dopaminergic neurons. J Comp Neurol 479:198–215. doi: 10.1002/cne.20323

Haggarty SJ, Perlis RH (2014) Translation: screening for novel therapeutics with disease-relevant cell types derived from human stem cell models. Biol Psychiatry 75:952–960. doi: 10.1016/j.biopsych.2013.05.028

Halliwell B (2006) Oxidative stress and neurodegeneration: where are we now? J Neurochem 97:1634–58. doi: 10.1111/j.1471-4159.2006.03907.x

Halperin I, Ma B, Wolfson H, Nussinov R (2002) Principles of docking: An overview of search algorithms and a guide to scoring functions. Proteins 47:409–43. doi: 10.1002/prot.10115

Hämmerle B, Yañez Y, Palanca S, et al (2013) Targeting neuroblastoma stem cells with retinoic acid and proteasome inhibitor. PLoS One 8:e76761. doi: 10.1371/journal.pone.0076761

Hanrott K, Gudmunsen L, O'Neill MJ, Wonnacott S (2006) 6-hydroxydopamine-induced apoptosis is mediated via extracellular auto-oxidation and caspase 3-dependent activation of protein kinase Cdelta. J Biol Chem 281:5373–82.

doi: 10.1074/jbc.M511560200

Hartfield EM, Yamasaki-Mann M, Ribeiro Fernandes HJ, et al (2014) Physiological characterisation of human iPS-derived dopaminergic neurons. PLoS One 9:e87388. doi: 10.1371/journal.pone.0087388

Herrup K, Yang Y (2007) Cell cycle regulation in the postmitotic neuron: oxymoron or new biology? Nat Rev Neurosci 8:368–78. doi: 10.1038/nrn2124

Howman-Giles R, Shaw PJ, Uren RF, Chung DK V (2007) Neuroblastoma and other neuroendocrine tumors. Semin Nucl Med 37:286–302. doi: 10.1053/j.semnuclmed.2007.02.009

Hsu M-F, Sun S-P, Chen Y-S, et al (2005) Distinct effects of N-ethylmaleimide on formyl peptide- and cyclopiazonic acid-induced Ca2+ signals through thiol modification in neutrophils. Biochem Pharmacol 70:1320–9. doi: 10.1016/j.bcp.2005.07.029

Http://www.genome.jp/kegg/pathway.html (2016) http://www.genome.jp/kegg/pathway.html.

Hu K, Carroll J, Rickman C, Davletov B (2002) Action of complexin on SNARE complex. J Biol Chem 277:41652–6. doi: 10.1074/jbc.M205044200

Iglesias-González J, Sánchez-Iglesias S, Méndez-Álvarez E, et al (2012) Differential toxicity of 6-hydroxydopamine in SH-SY5Y human neuroblastoma cells and rat brain mitochondria: protective role of catalase and superoxide dismutase. Neurochem Res 37:2150–60. doi: 10.1007/s11064-012-0838-6

Izumi Y, Sawada H, Sakka N, et al (2005) p-Quinone mediates 6-hydroxydopamine-induced dopaminergic neuronal death and ferrous iron accelerates the conversion of p-quinone into melanin extracellularly. J Neurosci Res 79:849–60. doi: 10.1002/jnr.20382

Kandel E (2013) Principles of Neural Science, Fifth Edition.

Korecka JA, van Kesteren RE, Blaas E, et al (2013) Phenotypic Characterization of Retinoic Acid Differentiated SH-SY5Y Cells by Transcriptional Profiling. PLoS One 8:e63862. doi: 10.1371/journal.pone.0063862

Kovalevich J, Langford D (2013) Considerations for the use of SH-SY5Y neuroblastoma cells in neurobiology. Methods Mol Biol 1078:9–21. doi: 10.1007/978-1-62703-640-5_2

Kunzler A, Zeidan-Chulia F, Gasparotto J, et al (2016) Changes in Cell Cycle and Up-Regulation of Neuronal Markers During SH-SY5Y

Neurodifferentiation by Retinoic Acid are Mediated by Reactive Species Production and Oxidative Stress. Mol Neurobiol. doi: 10.1007/s12035-016-0189-4

Lin C-Y, Tsai C-W (2016) Carnosic Acid Attenuates 6-Hydroxydopamine-Induced Neurotoxicity in SH-SY5Y Cells by Inducing Autophagy Through an Enhanced Interaction of Parkin and Beclin1. Mol Neurobiol. doi: 10.1007/s12035-016-9873-7

Ljungdahl A, Hökfelt T, Jonsson G, Sachs C (1971) Autoradiographic demonstration of uptake and accumulation of 3H-6-hydroxydopamine in adrenergic nerves. Experientia 27:297–9.

Lopert P, Day BJ, Patel M (2012) Thioredoxin reductase deficiency potentiates oxidative stress, mitochondrial dysfunction and cell death in dopaminergic cells. PLoS One 7:e50683. doi: 10.1371/journal.pone.0050683

Lopes FM, Londero GF, de Medeiros LM, et al (2012) Evaluation of the neurotoxic/neuroprotective role of organoselenides using differentiated human neuroblastoma SH-SY5Y cell line challenged with 6-hydroxydopamine. Neurotox Res 22:138–49. doi: 10.1007/s12640-012-9311-1

Lopes FM, Schröder R, da Frota MLC, et al (2010) Comparison between proliferative and neuron-like SH-SY5Y cells as an in vitro model for Parkinson disease studies. Brain Res 1337:85–94. doi: 10.1016/j.brainres.2010.03.102

Luchtman DW, Song C (2010) Why SH-SY5Y cells should be differentiated. Neurotoxicology 31:164–5; author reply 165–6. doi: 10.1016/j.neuro.2009.10.015

Madison JM, Nurrish S, Kaplan JM (2005) UNC-13 interaction with syntaxin is required for synaptic transmission. Curr Biol 15:2236–42. doi: 10.1016/j.cub.2005.10.049

Mohammad MK, Al-Masri IM, Taha MO, et al (2008) Olanzapine inhibits glycogen synthase kinase-3beta: an investigation by docking simulation and experimental validation. Eur J Pharmacol 584:185–91. doi: 10.1016/j.ejphar.2008.01.019

Olanow CW (2009) Can we achieve neuroprotection with currently available anti-parkinsonian interventions? Neurology 72:S59–64. doi: 10.1212/WNL.0b013e318199068b

Olanow CW, Kieburtz K, Schapira AH V (2008) Why have we failed to achieve neuroprotection in Parkinson's disease? Ann Neurol 64 Suppl 2:S101–10. doi: 10.1002/ana.21461

Påhlman S, Ruusala AI, Abrahamsson L, et al (1984) Retinoic acid-induced differentiation of cultured human neuroblastoma cells: a comparison with phorbolester-induced differentiation. Cell Differ 14:135–44.

Penmatsa A, Wang KH, Gouaux E (2013) X-ray structure of dopamine transporter elucidates antidepressant mechanism. Nature 503:85–90. doi: 10.1038/nature12533

Pezzini F, Bettinetti L, Di Leva F, et al (2016) Transcriptomic Profiling Discloses Molecular and Cellular Events Related to Neuronal Differentiation in SH-SY5Y Neuroblastoma Cells. Cell Mol Neurobiol 1–18. doi: 10.1007/s10571-016-0403-y

Policastro L, Molinari B, Larcher F, et al (2004) Imbalance of antioxidant enzymes in tumor cells and inhibition of proliferation and malignant features by scavenging hydrogen peroxide. Mol Carcinog 39:103–13. doi: 10.1002/mc.20001

Presgraves SP, Ahmed T, Borwege S, Joyce JN (2004) Terminally differentiated SH-SY5Y cells provide a model system for studying neuroprotective effects of dopamine agonists. Neurotox Res 5:579–98.

Qiao J, Paul P, Lee S, et al (2012) PI3K/AKT and ERK regulate retinoic acid-induced neuroblastoma cellular differentiation. Biochem Biophys Res Commun 424:421–6. doi: 10.1016/j.bbrc.2012.06.125

Radio NM, Mundy WR (2008) Developmental neurotoxicity testing in vitro: models for assessing chemical effects on neurite outgrowth. Neurotoxicology 29:361–76. doi: 10.1016/j.neuro.2008.02.011

Rizo J, Xu J (2015) The Synaptic Vesicle Release Machinery. Annu Rev Biophys 44:339–67. doi: 10.1146/annurev-biophys-060414-034057

Ross HJ (1996) The antiproliferative effect of trans-retinoic acid is associated with selective induction of interleukin-1 beta, a cytokine that directly inhibits growth of lung cancer cells. Oncol Res 8:171–8.

Schapira AH, Mann VM, Cooper JM, et al (1990) Anatomic and disease specificity of NADH CoQ1 reductase (complex I) deficiency in Parkinson's disease. J Neurochem 55:2142–5.

Schönhofen P, de Medeiros LM, Bristot IJ, et al (2015) Cannabidiol Exposure During Neuronal Differentiation Sensitizes Cells Against Redox-Active Neurotoxins. Mol Neurobiol 52:26–37. doi: 10.1007/s12035-014-8843-1

Schüle B, Pera RAR, Langston JW (2009) Can cellular models revolutionize drug discovery in Parkinson's disease? Biochim Biophys Acta 1792:1043–51. doi: 10.1016/j.bbadis.2009.08.014

Sharow KA, Temkin B, Asson-Batres MA (2012) Retinoic acid stability in stem cell cultures. Int J Dev Biol 56:273–278. doi: 10.1387/ijdb.113378ks

Sies H (2014) Role of metabolic H2O2 generation: redox signaling and oxidative stress. J Biol Chem 289:8735–41. doi: 10.1074/jbc.R113.544635

Soto-Otero R, Méndez-Alvarez E, Hermida-Ameijeiras A, et al (2000) Autoxidation and neurotoxicity of 6-hydroxydopamine in the presence of some antioxidants: potential implication in relation to the pathogenesis of Parkinson's disease. J Neurochem 74:1605–12.

Storch A, Kaftan A, Burkhardt K, Schwarz J (2000) 6-Hydroxydopamine toxicity towards human SH-SY5Y dopaminergic neuroblastoma cells: independent of mitochondrial energy metabolism. J Neural Transm 107:281–93.

Subramanian A, Tamayo P, Mootha VK, et al (2005) Gene set enrichment analysis: a knowledge-based approach for interpreting genome-wide expression profiles. Proc Natl Acad Sci U S A 102:15545–50. doi: 10.1073/pnas.0506580102

Takei K, Mundigl O, Daniell L, De Camilli P (1996) The synaptic vesicle cycle: a single vesicle budding step involving clathrin and dynamin. J Cell Biol 133:1237–50.

Tranzer JP, Thoenen H (1973) Selective destruction of adrenergic nerve terminals by chemical analogues of 6-hydroxydopamine. Experientia 29:314–5.

www.atcc.org/Products/All/CRL-2266.aspx www.atcc.org/Products/All/CRL-2266.aspx. http://www.atcc.org/Products/All/CRL-2266.aspx. Accessed 19 May 2016

Xie H, Hu L, Li G (2010) SH-SY5Y human neuroblastoma cell line: in vitro cell model of dopaminergic neurons in Parkinson's disease. Chin Med J (Engl) 123:1086–92.

Zhou ZD, Lan YH, Tan EK, Lim TM (2010) Iron species-mediated dopamine oxidation, proteasome inhibition, and dopaminergic cell demise: implications for iron-related dopaminergic neuron degeneration. Free Radic Biol Med 49:1856–71. doi: 10.1016/j.freeradbiomed.2010.09.010

Figure Captions

Fig 1 Protocol design of the RA-induced differentiation. At day 0, exponentially growing SH-SY5Y cells were cultured in cell medium containing 10% FBS. After 24 hours (day 1), the medium was removed and fresh medium containing 1% FBS and 10 µM RA (differentiation medium) was added. 3 days later (day 4), the differentiation medium was replaced with fresh differentiation medium. At day 7, SH-SY5Y cells were used in experiments

Fig. 2 Neuronal characterization of undifferentiated and RA-differentiated SH-SY5Y cells (A) Cellular growth in undifferentiated and RA-differentiated cells. (B) Cell cycle analysis. Representative image of the cell cycle analysis in undifferentiated cells and RA-differentiated cells, in which results were expressed as percentage of cells in each cell cycle phase (G0/G1, S, G2/M). Neurite density was evaluated by immunofluorescence. (C) Representative images of immunocytochemical detection of tubulin in undifferentiated and RA-differentiated SH-SY5Y cells. (D) Quantification of the neurite density per cell body using AutoQuant Neurite software. Expression of synaptic vesicle cycle network in undifferentiated and RA-differentiated SH-SY5Y cells. (E) STRING representation of synaptic vesicle cycle network gene interactions and landscape analysis, generated with ViaComplex® V1.0. Color gradient (Z-axis), demonstrating elevated expression of this network in 7-day-RA-differentiated, compared to undifferentiated, SH-SY5Y cells. *P* value refers to bootstrap analysis comparing cell lines. (F) Enrichment analysis used to identify the genes that contributed individually to the global changes in expression levels observed in RA-differentiated cells in the syntactic vesicle cycle network. Data are presented as mean ± SD of four independent experiments (n = 4), each carried

out in triplicates. *$P < 0.05$ (Student's *t*-test). Transcripts obtained as described in Material and Methods section. Nominal *p* value of enrichment analysis obtained from GSEA ($p < 0.05$)

Fig. 3 Dopaminergic characterization of undifferentiated and RA-differentiated SH-SY5Y cells. (A) Enrichment analysis used to identify the genes that contributed individually to the global changes in expression levels observed in RA-differentiated cells in the dopaminergic synapse network using GSEA. (B) Differential expression levels of pre-synaptic dopaminergic markers in undifferentiated and RA-differentiated cells. (C) Immunocytochemical detection of dopamine. Representative fluorescence microscopy images of undifferentiated and RA-differentiated SH-SY5Y cells. Data are presented as mean ± SD of four independent experiments (n = 4), each carried out in triplicates (n= 4). *$P < 0.05$ (Student's *t*-test).

Fig. 4 Redox characterization of undifferentiated and RA-differentiated SH-SY5Y cells. (A) Enrichment analysis used to identify the genes that contributed individually to the global changes in expression levels observed in RA-differentiated cells in the antioxidant network using GSEA. The role of cell-impermeable (B) and cell-permeable (D) thiol-reducing agents pre-treatment in 6-OHDA-induced cell death in undifferentiated and RA-differentiated SH-SY5Y cells. The results were expressed as a percentage of the control ± SD. Significant differences are expressed by *letters*, where *equal letters* represent no significant differences and *different letters* represent significant differences ($P < 0.05$) (one-way analysis of variance). (C,E) Analysis of the inhibition of 6-OHDA-induced cell death for each thiol-reducing agent in both cellular models.

Data are presented as mean ± SD of four independent experiments (n = 4), each carried out in triplicates. *$P < 0.05$ (Student's *t*-test)

Fig. 5 Evaluation of the role of DAT in 6-OHDA-induced cell death in undifferentiated and RA-differentiated SH-SY5Y cells (A) Changes in DAT immunocontent (dopaminergic cell marker) in response to RA-differentiation was evaluated using Western blot. Representative densitometric analysis of bands and immunoblot of DAT, using GAPDH as loading control. Results were calculated and expressed as mean ± SD of densitometric units (n = 4). *$P < 0.01$ (Student's *t*-test). (B) Superposition of DATi and 6-OHDA into the binding site of DAT, showing how 6-OHDA is spatially blocked from forming a salt bridge with Asp46. (C) Evaluation of DAT inhibition in the rate of H_2O_2 production, DAT-dependent H_2O_2 generation and (E) cell death in undifferentiated and RA-differentiated SH-SY5Y cells challenged with 6-OHDA. Cells were treated for 30 minutes with DATi prior to incubation with LD_{50} concentration of 6-OHDA for 24 hours. Cell viability was evaluated using the MTT reduction assay and results were expressed as percentage of untreated cells. Significant differences are expressed by *letters*, where *equal letters* represent no significant differences and *different letters* represent significant differences ($P < 0.05$) (one-way analysis of variance). (D,F) DAT-dependent 6-OHDA-induced cell death in both cellular models. Data are presented as mean ± SD of four independent experiments, each carried out in triplicates (n=4). *$P < 0.05$ (Student's *t*-test)

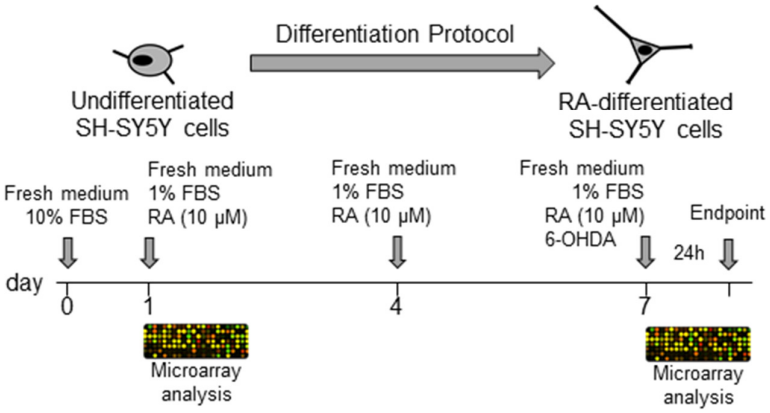
Differentiation Protocol
Undifferentiated
SH-SY5Y cells
RA-differentiated
SH-SY5Y cells
Fresh medium
10% FBS
Fresh medium
1% FBS
RA (10 µM)
Fresh medium
1% FBS
RA (10 µM)
Fresh medium
1% FBS
RA (10 µM)
6-OHDA
Endpoint
24h
day
0
1
4
7
Microarray
analysis
Microarray
analysis

Figure 1

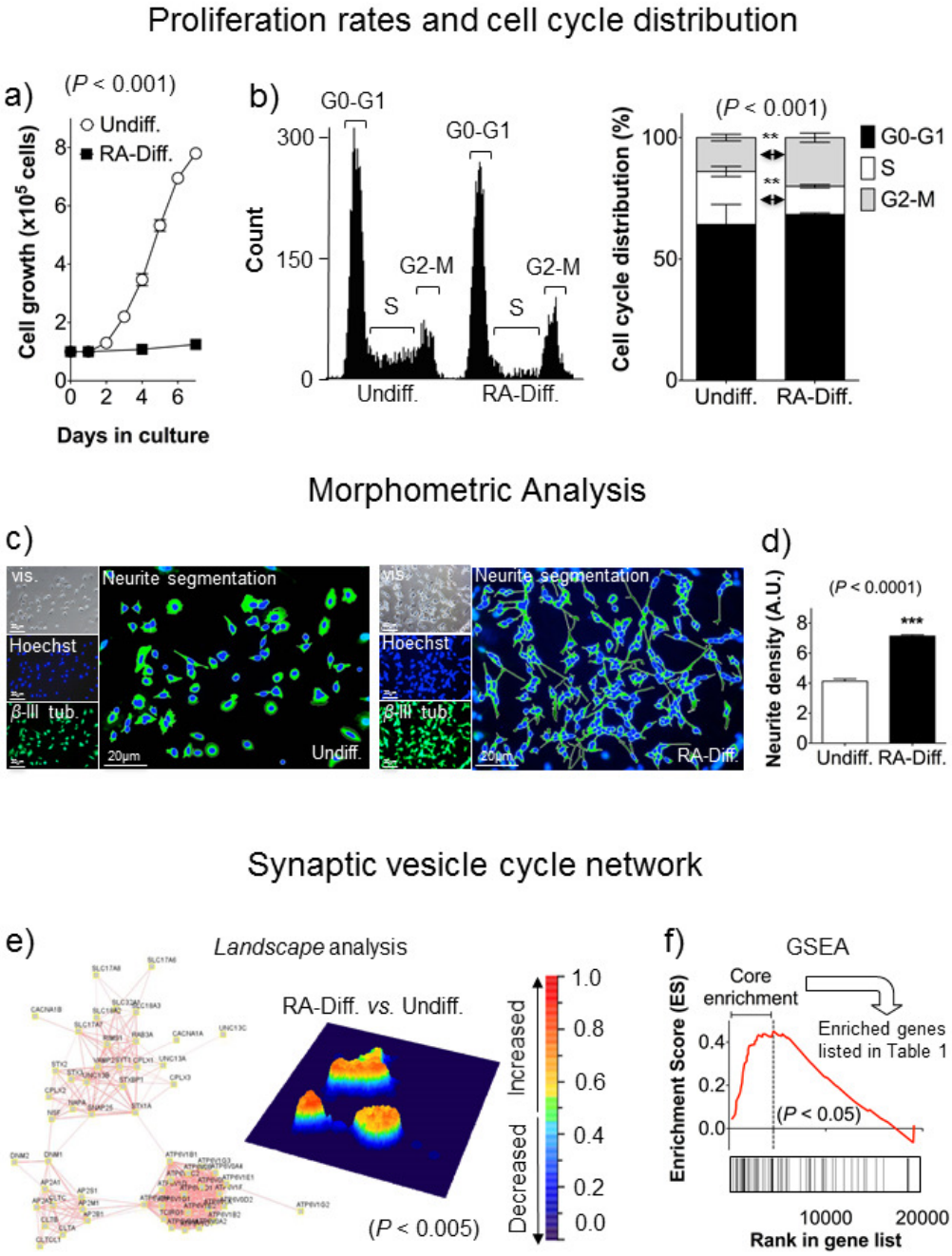
Proliferation rates and cell cycle distribution
a)
(P < 0.001)
Undiff.
RA-Diff.
Cell growth (x10^5 cells)
Days in culture
b)
G0-G1
G2-M
S
Count
Undiff.
RA-Diff.
(P < 0.001)
Cell cycle distribution (%)
G0-G1
S
G2-M
Morphometric Analysis
c)
vis.
Hoechst
β-III tub.
Neurite segmentation
20μm
Undiff.
RA-Diff.
d)
(P < 0.0001)
Neurite density (A.U.)
Undiff. RA-Diff.
Synaptic vesicle cycle network
e)
Landscape analysis
RA-Diff. vs. Undiff.
(P < 0.005)
Increased
Decreased
f)
GSEA
Core enrichment
Enriched genes listed in Table 1
Enrichment Score (ES)
(P < 0.05)
Rank in gene list

Figure 2

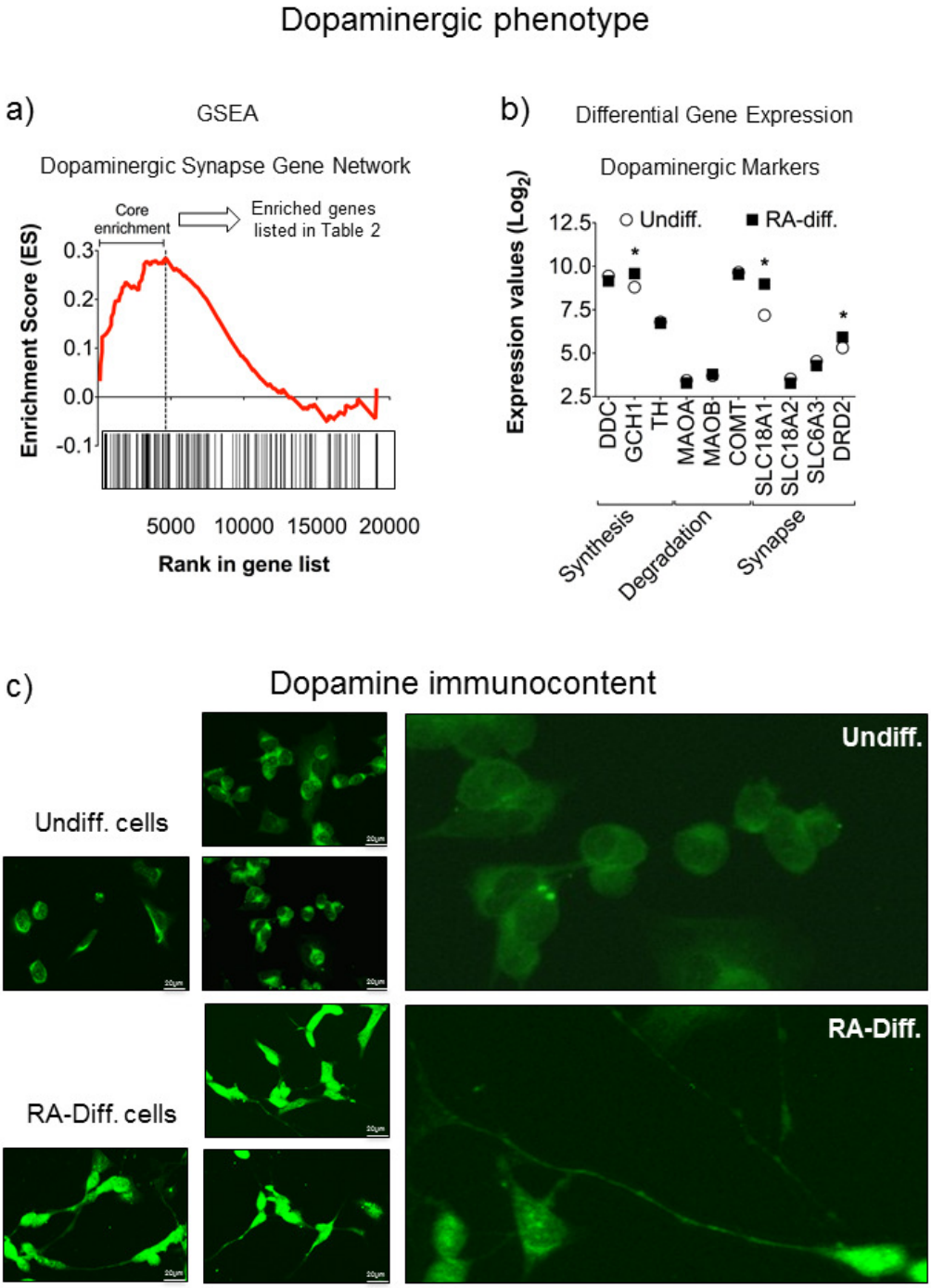
Dopaminergic phenotype
a)
GSEA
Dopaminergic Synapse Gene Network
Core enrichment
Enriched genes listed in Table 2
Enrichment Score (ES)
0.3
0.2
0.1
0.0
-0.1
5000
10000
15000
20000
Rank in gene list
b)
Differential Gene Expression
Dopaminergic Markers
Expression values (Log2)
Undiff.
RA-diff.
12.5
10.0
7.5
5.0
2.5
DDC
GCH1
TH
MAOA
MAOB
COMT
SLC18A1
SLC18A2
SLC6A3
DRD2
Synthesis
Degradation
Synapse
c)
Dopamine immunocontent
Undiff. cells
RA-Diff. cells
Undiff.
RA-Diff.

Figure 3

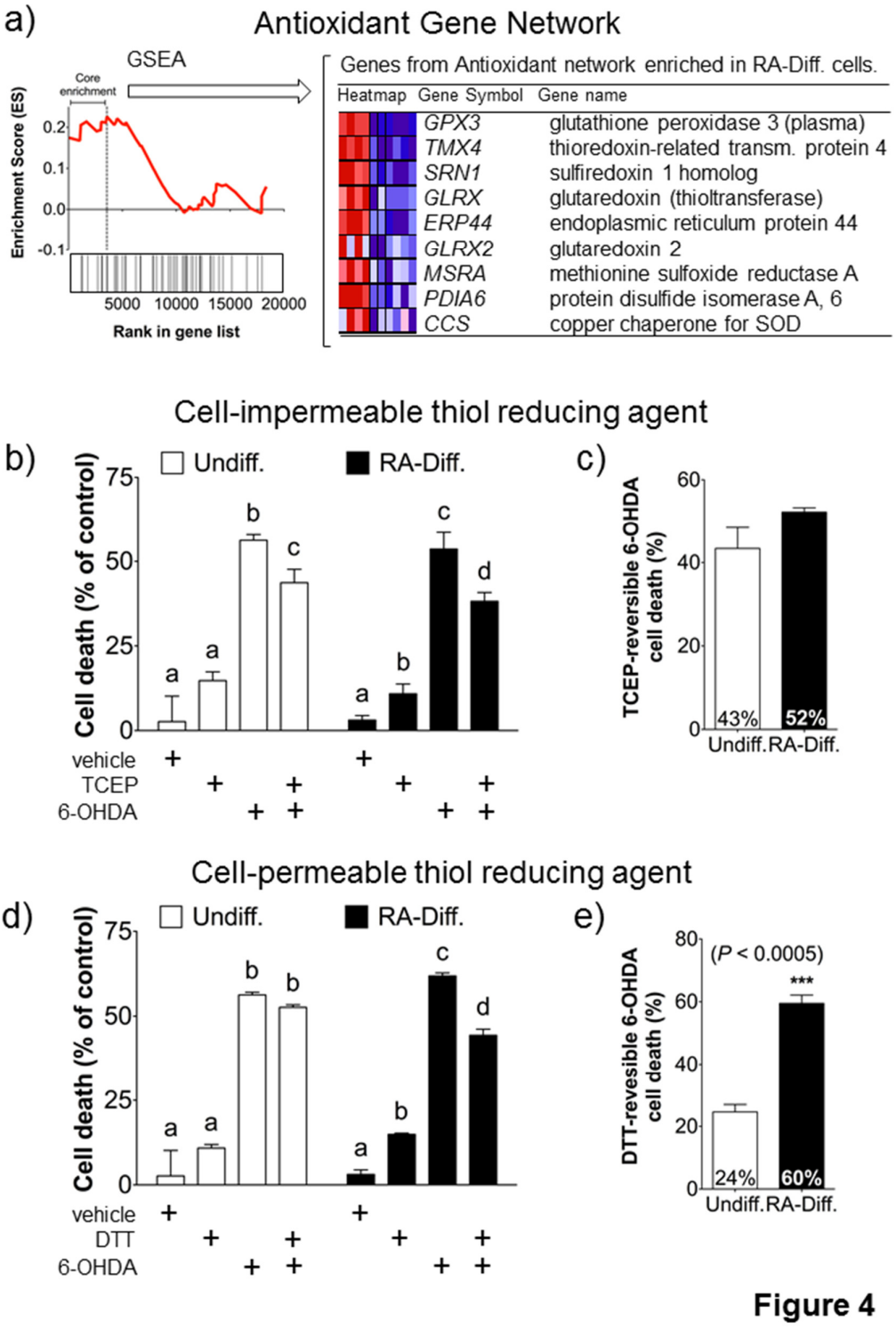
a)
Antioxidant Gene Network
GSEA
Core enrichment
Enrichment Score (ES)
0.2
0.1
0.0
-0.1
5000 10000 15000 20000
Rank in gene list
Genes from Antioxidant network enriched in RA-Diff. cells.
Heatmap Gene Symbol Gene name
GPX3 glutathione peroxidase 3 (plasma)
TMX4 thioredoxin-related transm. protein 4
SRN1 sulfiredoxin 1 homolog
GLRX glutaredoxin (thioltransferase)
ERP44 endoplasmic reticulum protein 44
GLRX2 glutaredoxin 2
MSRA methionine sulfoxide reductase A
PDIA6 protein disulfide isomerase A, 6
CCS copper chaperone for SOD
Cell-impermeable thiol reducing agent
b)
Undiff.
RA-Diff.
Cell death (% of control)
75
50
25
0
a a b c a b c d
vehicle + + + +
TCEP + + + +
6-OHDA + + + +
c)
TCEP-reversible 6-OHDA cell death (%)
60
40
20
0
43%
52%
Undiff. RA-Diff.
Cell-permeable thiol reducing agent
d)
Undiff.
RA-Diff.
Cell death (% of control)
75
50
25
0
a a b b a b c d
vehicle + + + +
DTT + + + +
6-OHDA + + + +
e)
DTT-revesible 6-OHDA cell death (%)
80
60
40
20
0
(P < 0.0005)
***
24%
60%
Undiff. RA-Diff.

Figure 4

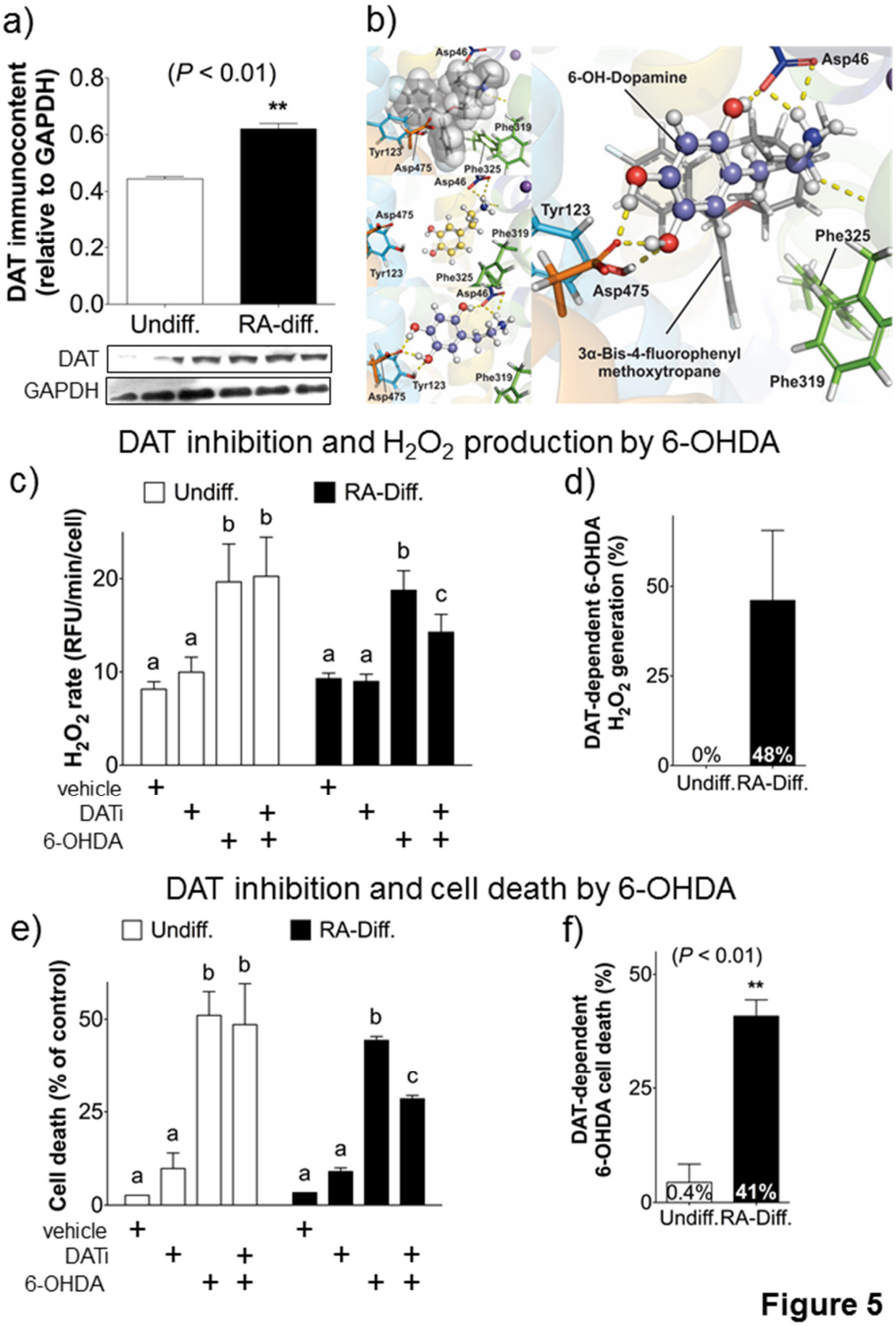
a)
b)
DAT immunocontent (relative to GAPDH)
(P < 0.01)
**
Undiff.
RA-diff.
DAT
GAPDH
6-OH-Dopamine
Asp46
Tyr123
Asp475
Phe325
Phe319
3α-Bis-4-fluorophenyl methoxytropane
DAT inhibition and H2O2 production by 6-OHDA
c)
d)
Undiff.
RA-Diff.
H2O2 rate (RFU/min/cell)
vehicle
DATi
6-OHDA
DAT-dependent 6-OHDA H2O2 generation (%)
0%
48%
DAT inhibition and cell death by 6-OHDA
e)
f)
Cell death (% of control)
DAT-dependent 6-OHDA cell death (%)
0.4%
41%

Figure 5